

METHOD AND APPARATUS TO DETERMINE THE MONOCHROMATIC NORMALLY  
HEMISPHERICAL REFLECTIVITY OF HEAT-SHIELD MATERIALS

L. S. Slobodkin, M. Ya. Flyaks,  
and B. V. Andreev

UDC 536.3:535.312

A method and apparatus are described for the determination of the monochromatic normally hemispheric reflectivity  $\rho_{\lambda n}$ ; results of measuring  $\rho_{\lambda n}$  for a number of composite materials are presented.

Knowledge of the thermal radiation characteristics of heat-shield material (HSM) is necessary to solve problems of the heat and mass transfer of surfaces covered with heat-shield materials (HSM), and therefore for the analysis and design of structures and apparatus subjected to intensive heat loads. One of the most important characteristics in practice is the spectral directional emissivity  $\epsilon_{\lambda\alpha}$ . The experimental determination of  $\epsilon_{\lambda\alpha}$  is most often realized by means of the results of comparing specimen and standard radiation [1]. The main disadvantage of this method is that the accuracy of determining  $\epsilon_{\lambda\alpha}$  depends strongly on the accuracy of determining the true temperature of the surface being inspected, especially in the shortwave range. This circumstance turns out to be quite essential in application to HSM, which as a rule possess low values of the heat-conduction coefficient, and, consequently, substantial temperature gradients over the specimen. The difficulties associated with the determination of the true temperature of the surface being inspected can be eliminated in a measurement of the monochromatic directional hemispherical reflectivity  $\rho_{\lambda\alpha}$  at a given wavelength, and the subsequent determination of  $\epsilon_{\lambda\alpha}$  at this same wavelength by means of Kirchhoff's law. In the rest of the spectrum range,  $\epsilon_{\lambda\alpha}$  can hence be found by the method of comparing with the standard.

Different schemes based on arc elliptical reflectometers (see [2, 3] e.g.) are used most often to measure the  $\rho_{\lambda\alpha}$  of materials at high temperatures. Hence, the reflected and intrinsic radiation are separated by using modulation of the radiant flux incident on the specimen. The integrating sphere is usually used for investigations in the low and moderate temperature range [4], but it is used sufficiently rarely [1] for measurements at high temperatures, although, as a rule, the application of an integrating sphere permits diminution of the size, and substantially simplifies the apparatus.

A method and apparatus to determine  $\rho_{\lambda n}$  are described below, which provide for the use of an integrating sphere, laser heating of the specimen, and visual determination of the reflectivity (by a brightness pyrometer scheme). One of the advantages of using laser radiation is the fact that small sections of the specimen surface are subjected to heating. Consequently, the process of contamination of the optical elements (sphere, window surfaces, etc.) occurs less intensively for ablating materials. The circumstance is also essential that the need to take account of the radiation of the heating source reflected by the specimen drops out when a laser beam is used, as is required when using continuous-spectrum sources (e.g., xenon arc lamps, etc.) [5]. Visual determination of the brightness of an object permits measurement of the  $\rho_{\lambda n}$  of sufficiently small surface sections, particularly the structural elements of composite materials, and also of conducting a fast qualitative estimate of the change in the properties of the material and its components during the heating. Utilization of this method and apparatus in an aggregate with the stand and method described in [6, 7] is provided for in determining the normal spectral emissivity.

The diagram of the apparatus intended to determine the normal hemispherical reflectivity of heat-shield materials in the visible spectrum range at the wavelengths  $\lambda = 0.58, 0.546$  and  $0.436 \mu\text{m}$  is shown in Fig. 1. Its main elements are the chamber 1, executing the role of the integrating sphere, two LG-22 CO<sub>2</sub> type lasers 2 used to heat the specimen section being inspected, and the measuring instrument 3. Radiation sources 4 with a ruled spectrum (two

---

A. V. Lykov Institute of Heat and Mass Transfer, Academy of Sciences of the Belorussian SSR, Minsk. Translated from *Inzhenerno-Fizicheskii Zhurnal*, Vol. 42, No. 3, pp. 442-448, March, 1982. Original article submitted December 29, 1980.

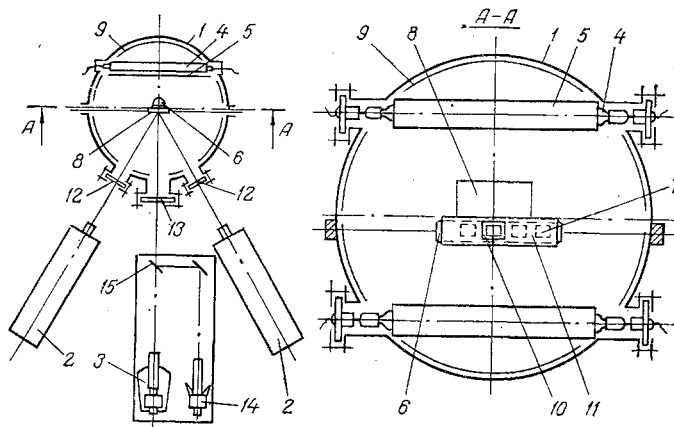


Fig. 1. Diagram of the apparatus to determine  $\rho_{\lambda n}$ .

lamps of DRT-375 type), reflectors 5 hindering the direct incidence of radiation from the lamps on the forward hemisphere, a mobile cassette 6 with gaps 7 filled with the standard coating, and the specimen 8 are within the space of the chamber 1. The inner surface of the chamber is a sphere of 240-mm diameter coated with a diffuse reflecting material [barium sulfate ( $\text{BaSO}_4$ )]. Magnesium oxide ( $\text{MgO}$ ), which was deposited in the gap 7 of the cassette 6 during the ignition of metallic magnesium, was used as the standard coating. The surface of the sphere is contaminated by decomposition products when specimens from decomposing materials are heated. In order to deposit new coatings more rarely, two hemispheres 9 from 2-mm-thick Pyrex are inserted in the sphere, where their outer surface is coated with  $\text{BaSO}_4$ . The inner surface of the hemisphere is periodically wiped clean. To eliminate the possibility of contamination of the standard surface, the cassette 6 is made mobile. At the instant of the measurement the cassette is displaced in such a manner that the gap with the standard coating would appear in the window 10 of the cover 11. As was already noted, the specimen is heated by a beam of laser radiation at the wavelength  $\lambda = 10.6 \mu\text{m}$  which is inserted into the sphere through the window 12 fabricated from NaCl. The specimen and standard are inspected through the quartz window 13 by means of the measuring instrument 3. To determine the brightness temperature at the wavelength  $\lambda = 1.02 \mu\text{m}$  in the  $T = 400\text{--}800^\circ\text{C}$  temperature range, a VIMP-015M pyrometer 14 is used. Observation of the standard is assured in this case by using the mobile flat mirrors 15.

The radiant flux being recorded during inspection of the specimen is comprised of two components, the intrinsic and reflected radiation. The reflectivity can be determined from the relationship

$$\rho_{\lambda n} = \frac{I_s - I_0}{I_b} = R_s - R_0, \quad (1)$$

where  $R_s = I_s/I_b$ ,  $R_0 = I_0/I_b$ .

Construction of the measuring device 3 permits determination of the specimen and standard brightness with subsequent measurement of the relative brightnesses  $R_s$  and  $R_0$ . The specimen brightness due to the total intrinsic and reflected radiation is determined at the wavelength  $\lambda_i$  of DRT-375 lamp emission, and the intensity of the intrinsic radiation at the length  $\lambda_j$  near  $\lambda_i$ . Hence it is assumed that because of the closeness of the values  $\lambda_i$  and  $\lambda_j$ , the equality  $\epsilon_{\lambda_i n} = \epsilon_{\lambda_j n}$  is conserved. It should be noted that this method does not require switching off the lamp to determine  $R_0$ , permitting sufficiently rapid measurement, in turn, of the parameters needed by eliminating thereby the influence of specimen temperature drift caused by instability of the laser beam. The following circumstance also plays a substantial part: A long cool-off time (on the order of 30 min) after switch-off and the emergence into a stable mode after the second switch-on are required for the DRT-375 lamps under the conditions for this chamber. Hence, elimination of the need for switching off the lamps shortens the measurement time and affords a possibility for their duplication, thereby assuring high confidence in the results.

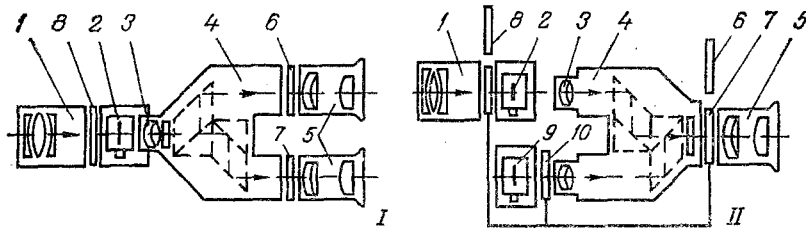


Fig. 2. Diagram of the measuring device unit I, modification II.

The diagrams of two versions of the measuring device unit, executed on the basis of the etalon optical pyrometer ÉOP-66, are represented in Fig. 2. The telescope 1 is used to project the image of the object in the plane of the pyrometric lamp wire 2. Observation of the wire and the object in version I of the device is by means of the microobjective 3, the binocular cap 4, and the oculars 5 with the total 30× enlargement. Light filter No. 1 (6) permits examining the object and the wire at the wavelength  $\lambda_i$ , and light filter No. 2 (7) permits examination at the wavelength  $\lambda_j$ . The attenuating glasses mounted in the cassette 8 are to diminish the object brightness being observed to a given level. The measurement process is the sequential determination of the standard brightness at the wavelength  $\lambda_i$ , and the specimen brightness at the wavelengths  $\lambda_i$  and  $\lambda_j$ . The passage to the ratios  $R_s = I_s/I_b$  and  $R_o = I_o/I_b$  is accomplished as follows. Before beginning the measurements, the pyrometric lamps are calibrated. During the calibration, glasses with known transmission are placed alternately in the cassette 8 for examination of the standard, and the standard brightness is measured. Two brightnesses are compared by this means, or equivalently, two values of the current in the pyrometer lamp wire, the initial without attenuation, and the given current in the presence of an absorber with known transmissivity. The ratio of the intensities of the corresponding radiant fluxes here equals the transmission factor of the attenuating glass. In performing the intrinsic measurements, the brightness being observed for the standard is changed to the initial standard brightness during the calibration by inserting an additional absorber. Then by measuring the object brightness at the wavelengths  $\lambda_i$  and  $\lambda_j$ , we obtain values of  $R_s$  and  $R_o$  in conformity with the calibration. The quantity  $R_s$  is determined during inspection of the specimen and standard in the spectrum band  $\lambda_i$ , and  $R_o$  during specimen inspection at the length  $\lambda_j$  and the standard in the band  $\lambda_i$ .

$$R_s(\lambda_i) = \frac{I_s(\lambda_i)}{I_b(\lambda_i)}, \quad R_o(\lambda_j) = \frac{I_o(\lambda_j)}{I_b(\lambda_j)}, \quad (2)$$

$$\rho_{\lambda_i n} = R_s(\lambda_i) - R_o(\lambda_j). \quad (3)$$

It is hence assumed that the emissivities of the pyrometric lamp wires are identical at the wavelengths  $\lambda_i$  and  $\lambda_j$ . Relationship (3) is true in the absence of background in the band  $\lambda_j$ . However, in reality it is desirable to select  $\lambda_j$  as close as possible to  $\lambda_i$ . Here the appearance of a background is possible in the band  $\lambda_j$ , which is associated with the presence of a definite filter transmission at the length  $\lambda_i$  and a continuous component of the DRT-375 lamp radiation spectrum at the wavelength  $\lambda_j$ . In this case  $\rho_{\lambda_i n}$  is determined by the formula

$$\rho_{\lambda_i n} = \frac{R_s(\lambda_i) - R_s(\lambda_j)}{1 - R_b(\lambda_i, \lambda_j)}, \quad (4)$$

where

$$R_b = \frac{I_b(\lambda_j)}{I_b(\lambda_i)}, \quad R_s(\lambda_j) = \frac{I_s(\lambda_j)}{I_b(\lambda_i)}.$$

Upon substituting

$$I_s(\lambda_j) = I_o(\lambda_j) + \rho_{\lambda_i n} I_b(\lambda_j),$$

this relationship reduces to (3).

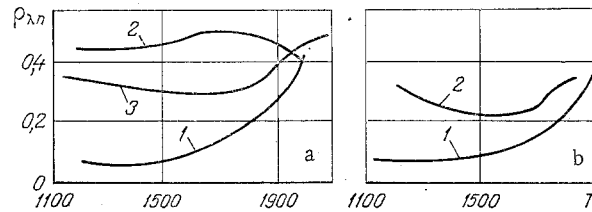


Fig. 3. Change in the normally hemispherical reflectivity  $\rho_{\lambda n}$  at the wavelength  $\lambda = 0.58 \mu\text{m}$  as a function of the temperature  $T$ ,  $^{\circ}\text{K}$ : a) Specimen No. 1 [1) before treatment; 2, 3) after treatment in a plasma flux; 2) specimen thickness  $h = 3.6 \text{ mm}$ , 3)  $4.7 \text{ mm}$ ]; b) No. 2 [1) before treatment; 2) after treatment].

The measurements were performed in the following order. Since the radiation of the DRT-375 lamp is sufficiently stable, the etalon brightness is measured first at the wavelengths  $\lambda_i$  and  $\lambda_j$ , and then a rapid measurement of the specimen brightness is made in these bands. The time interval between the two observations is here determined principally by the inertia of the wire. The main error in this case occurs because of the possible drift of the specimen surface temperature during the measurements of  $I_s(\lambda_i)$  and  $I_s(\lambda_j)$ .

This source of error in the determination of  $\rho_{\lambda n}$  is eliminated to a significant extent by using modification II of the measuring device. The binocular cap 4 with two microobjectives 3 and ocular 5 is mounted in such a manner that the images of the pyrometric lamp wires 2 and 9 are superposed. The light filter No. 2 is set in the ocular when sighting the object at the wavelength  $\lambda_j$ , and the wire of the pyrometric lamp 9 is covered by the shutter 10. The  $I_s(\lambda_j)$  is measured by equilibrating the brightnesses of the wire of lamp 2 and the object. Filter No. 1 is mounted in the ocular when observing the object at the wavelength  $\lambda_i$ , and the wire of lamp 9 is opened for the sighting. The measurement of  $I_s(\lambda_i)$  is by equilibrating the total brightness of the two wires and of the specimen, which is achieved by changing the brightness of the wire of lamp 9 while keeping the brightness of the wire of lamp 2 unchanged. The advantage of such a measurement scheme is that the brightness of the wire of lamp 9 equals the brightness of the reflected radiation, which is practically invariant under small temperature fluctuations because of the weak dependence of  $\rho_{\lambda n}$  on  $T$ . Therefore, only the brightness of the wire of lamp 2 varies as the specimen temperature drifts, while the brightness of the wire of lamp 9 remains unchanged. A sufficiently accurate determination of the reflected radiation intensity is assured by performing several successive measurements with subsequently taking the average. The value of  $\rho_{\lambda_{in}}$  is found from the relationship

$$\rho_{\lambda n} = \frac{\Delta I_s(\lambda_i, \lambda_j)}{I_b(\lambda_i) [1 - R_b(\lambda_i, \lambda_j)]}, \quad (5)$$

where  $\Delta I_s(\lambda_i, \lambda_j) = I_s(\lambda_i) - I_s(\lambda_j)$  is the brightness of the wire of lamp 9.

The use of any modification of the measuring device is governed by the nature of the material being investigated and by its behavior in the temperature range under investigation. In the case of melting or thermal decomposition of the material or of one of its components, the radiant flux density fluctuations in the laser beam will not result in substantial temperature fluctuations of the specimen surface since the excess heat goes mainly into intensification of the process and not into raising the temperature. On the other hand, in this case a change in  $\rho_{\lambda n}$  with time is also possible at constant temperature. Consequently, the utilization of modification I is preferable in this case. Modification II is convenient for the investigation of nondecomposing materials, especially with low heat conductivity, because of the fact that by its use the error associated with temperature fluctuations is eliminated to a significant extent.

The order of calibrating the measuring device and performing the measurements that have been described above assumes that  $I_b > I_s$ . Taking this circumstance into account, the apparatus permits executing the measurements at the wavelengths  $\lambda = 0.58$  and  $0.546 \mu\text{m}$  to the temperature  $T \sim 2000^{\circ}\text{K}$ , and at the wavelength  $\lambda = 0.436 \mu\text{m}$  to the temperature  $T \sim 2300^{\circ}\text{K}$ .

Results of determining the  $\rho_{\lambda n}$  of a number of composite materials are presented in Fig. 3 as an illustration. The  $\rho_{\lambda n}$  were measured at the wavelength  $\lambda = 0.58 \mu\text{m}$  (two radiation lines of mercury vapor  $\lambda = 0.577$  and  $0.579 \mu\text{m}$ ). The corresponding spectrum band was extracted by a set of colored optical glasses OS-13, ZS-7, and SZS-23 of 5-mm thickness. The band parameters are the following: maximum transmission wavelength  $\lambda_{\text{max}} = 0.573 \mu\text{m}$ , width at the center of the maximum  $\Delta = 0.022 \mu\text{m}$ , and transmission  $\tau_{\text{max}} = 31\%$ . To measure the specimen intrinsic radiation intensity we used a light filter obtained by a combination of the interference light filter  $\lambda_{\text{max}} = 0.60 \mu\text{m}$ ,  $\Delta = 0.008 \mu\text{m}$ ,  $\tau_{\text{max}} = 32\%$  and the correction filter from KS-10 glass 5 mm thick. The filter transmission at the wavelength  $\lambda = 0.60 \mu\text{m}$  was  $\tau = 17\%$  while the relative transmission (with respect to  $\tau$  at  $\lambda = 0.60 \mu\text{m}$ ) did not exceed 0.1% for  $\lambda < 0.585 \mu\text{m}$ . The intensity of the continuous component of the DRT-375 lamp spectrum for  $\lambda = 0.60 \mu\text{m}$  did not exceed 1% of the background brightness at  $\lambda = 0.58 \mu\text{m}$ . In this connection, the relation (3) was used to calculate  $\rho_{\lambda n}$ . The measuring device in modification I was used to perform the measurements.

The  $\rho_{\lambda n}$  was determined both before and after treating the specimens being investigated in a gas-flame flux. As follows from Fig. 3, growth of  $\rho_{\lambda n}$  with temperature was observed for specimens Nos. 1 and 2 not subjected to preliminary treatment in the plasma jet. For specimens Nos. 1 and 2 which had been treated in the plasma jet,  $\rho_{\lambda n}$  varies insignificantly with the rise in temperature. Curves 2 and 3 in Fig. 3 correspond to reflectivity values for specimens of different thickness. Their difference is apparently explained by the dissimilar nature of specimen heating in the gas-flame jet. As follows from the results obtained, a substantial difference in the values of  $\rho_{\lambda n}$  is observed for specimens subjected and not subjected to treatment in a gas-flame flux. The data obtained for  $\rho_{\lambda n}$  were utilized in determining the  $\epsilon_{\lambda n}$  of HSM in the spectrum range  $\lambda = 0.4\text{--}10 \mu\text{m}$ ; however, the exposition of these results is beyond the scope of this paper and will be presented in a separate publication.

It must be noted that the determination of  $\epsilon_{\lambda n}$  in the visible domain can be carried out directly on the apparatus described. By extracting the given spectral sections by using filters, and by measuring the brightness temperature of the object therein, and then using the value of the true temperature of the surface being sighted,  $\epsilon_{\lambda n}$  can be determined. The true surface temperature is here determined during inspection of the specimen at the wavelength  $\lambda_i$  with the sources switched off and utilization of the values obtained earlier for  $\rho_{\lambda_i n}$ .

#### NOTATION

$\epsilon_{\lambda\alpha}$ ,  $\epsilon_{\lambda n}$ , directional and normal spectral emissivities, respectively;  $\rho_{\lambda\alpha}$ ,  $\epsilon_{\lambda n}$ , directional hemispheric and normally hemispheric spectral reflectivities, respectively;  $I_s$ , total intensity of intrinsic and reflected radiation;  $I_0$ , intensity of intrinsic specimen radiation;  $I_b$ , background brightness (intensity of radiation reflected from the standard);  $R_s$ ,  $R_0$ , relative brightnesses (relative to the background), respectively assured by the specimen total and intrinsic radiation;  $R_b$ , background brightness ratio with wavelength  $\lambda_i$  and  $\lambda_j$ ;  $\lambda_i$ , radiation wavelength of the source;  $\lambda_j$ , wavelengths at which the specimen intrinsic radiations are measured;  $\lambda_{\text{max}}$ ,  $\tau_{\text{max}}$ , wavelength of the maximum transmission and magnitude of the maximum transmission;  $\Delta$ , band width (at the center of the maximum).

#### LITERATURE CITED

1. L. N. Latyev et al., Emissivities of Solid Materials [in Russian], Énergiya, Moscow (1974).
2. N. A. Rubtsov and A. G. Tarasov, "Emissivities of crystal-oriented pyrolytic graphite at high temperatures," *Izv. Sib. Otd. Akad. Nauk SSSR, Ser. Tekh.*, No. 8, Issue 2, 8-12 (1977).
3. R. G. Wilson and K. R. Spitzer, "Emissivity of certain heat-shield material in the visible and near-infrared spectrum ranges," *Raket. Tekh. Kosmon. (AIAA J.)*, No. 4, 108-117 (1968).
4. S. G. Il'yasov and V. V. Krasnikov, *Methods of Determining the Optical and Thermal Radiation Characteristics of Food Products* [in Russian], Pishch. Prom-st' (1972).
5. S. A. Kats, V. Ya. Chekhovskii, and A. E. Sheindlin, "Investigation of the temperature dependence of the emissivity of liquid refractory metals," *Thermophysical Properties of Substances at High Temperatures* [in Russian], *Inst. Vys. Temp. Akad. Nauk SSSR, Moscow* (1978), pp. 81-94.
6. L. S. Slobodkin, M. Ya. Flyaks, and B. V. Andreev, "Method and apparatus to determine the emissivity of heat-shield materials," *Theory and Technique of Drying Moist Materials* [in Russian], A. V. Lykov *Inst. Teplo. Massoobmena Akad. Nauk BSSR, Minsk* (1979), pp. 16-29.

7. L. S. Slobodkin and M. Ya. Flyaks, "Development of a set of apparatus to determine the emissivity of heat-shield materials," Heat and Mass Transfer: Physical Principles and Methods of Investigations [in Russian], A. V. Lykov Inst. Teplo. Massoobmena Akad. Nauk BSSR, Minsk (1980), pp. 106-108.

#### EFFECTS OF RADIATION ON THERMAL CONDUCTIVITY OF SOME POLYMER RESINS

B. A. Briskman and S. I. Rozman

UDC 678.742:046

A study was made concerning the effect of radiation on the thermal conductivity of grade VK-9 adhesive (consisting of epoxy and polyamide resins) and of a "Kriosil" compound based on silicone resin.

A study was made to determine the effect of radiation on the thermal conductivity  $\lambda$  of the grade VK-9 polymer adhesive and the "Kriosil" compound. The former is a compound of grade ED-20 epoxy resin (60 wt.%) and grade PO-300 polyamide resin (40 wt.%). The initial density of this polymer is 1.04 g/cm<sup>3</sup> at 20°C. The "Kriosil" compound consists of grade DFMK<sub>r</sub> silicone resin (45 wt.%), grade L-20 low-molecular-weight polyamine (25 wt.%), boron nitride, and Aerosil. The density of this material is 1.20 g/cm<sup>3</sup>.

Method of Irradiation and Thermal Conductivity Measurement. Test specimens of these materials were produced in the form of disks 15 mm in diameter and 1.5-2.5-mm thick. They were irradiated in air with  $\gamma$  quanta in doses up to 0.01 and 1 MGy from a <sup>60</sup>Co source (dose power 3 Gy/sec) as well as with mixed  $\gamma$ -neutron flux in doses to 1, 3, 10, and 20 MGy from a nuclear reactor (dose power 11 Gy/sec). The irradiation temperature was 30°C for the <sup>60</sup>Co source and 50°C for the reactor channel.

In order to check for the possibility of radiation effects depending on the kind of radiation, irradiation in the reactor to 1 and 3 MGy was effected in core channels where fast neutrons  $m$  amounted to 50-60% of the dose absorbed by polyethylene. Irradiation to doses of 10 and 20 MGy was effected in reflector channels with  $m \sim 5\%$ .

The thermal conductivity was measured with model IT- $\lambda$ -400 instruments operating in the mode of monotonic heating at a rate of approximately 6°C/min, at temperatures from -100 to +180°C for the VK-9 adhesive and from -110 to +220°C for the Kriosil. The systematic error of measurements was 4-6%; the reproducibility of results was within 3%.

Grade VK-9 Adhesive. The thermal conductivity of grade VK-9 adhesive, based on the results of this study, is shown in Fig. 1 as a function of the temperature and in Fig. 2 as a

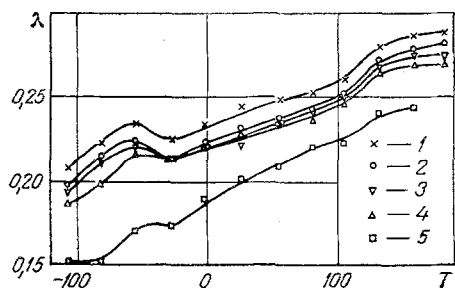


Fig. 1

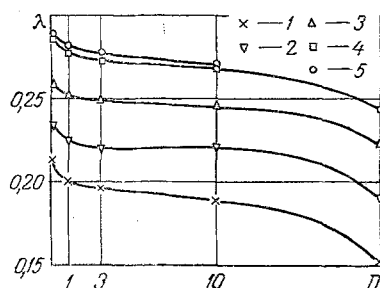


Fig. 2

Fig. 1. Temperature dependence of the thermal conductivity of grade VK-9 adhesive:  $\lambda$  (W/m·K),  $T$  (°C), with irradiation dose as parameter: 1) 0; 2) 1; 3) 3; 4) 10; 5) 20 MGy.

Fig. 2. Dependence of the thermal conductivity of grade VK-9 adhesive on the absorbed radiation dose,  $\lambda$  (W/m·K),  $D$  (MGy), with test temperature as parameter: 1) -100; 2) 0; 3) 100; 4) 150; 5) 180°C.